Supercapacitor Assisted Surge Absorber Technique for High Performance Transient Surge Protectors for Consumer Electronics

by Jayathu Fernando, Nihal Kularatna, Shanima Silva and Sadeeshvara Silva Thotabaddadurage

xxxxxx

Introduction

Invention of the transistor in 1947 made a radical change to the path of the development of electronic products and systems. In the mid-1950s, integrated circuits (ICs) started evolving rapidly, creating miniaturized analog, digital and mixed signal circuits. By the 1960s to 1970s, microprocessors, memories and power semiconductors entered the electronic marketplace. During the 1980s and 1990s, power supplies required to power the high-performance digital circuits kept dropping towards 2 V and below. By the year 2000, complex digital and mixed- signal circuits required for portable gadgets were powered by very low dc rails as low as 1 V and sub 1 V. Very large-scale ICs and ultra-large scale ICs proliferated after 2000, integrating millions to billions of sub-micron feature transistors. The ultimate result of this massive progress came with the unique problem of vulnerability of modern electronics to transient surges. A detailed background to this is presented in Chapter 1 of reference [1].

Figure 1(a) provides a pictorial view of transients and noise present on a 230 V 50 Hz utility ac power, and Figure 1(b) depicts the difference between differential mode and common mode transient voltage sources superimposed on the ac mains and the associated ground connection.

Circuit Designer's View to Surge Protectors

All surge protector devices (SPD) basically work on the simple concept of voltage divider [2]. Figure 2 illustrates this concept in three steps. In Figure 2(a), the superimposed surge appears on the load represented by Z_L based on the voltage division network comprising the compound series impedance Z_S and the value of Z_L. For the transient high voltage surge to have a minimal effect on the load represented by Z_L, ohmic value of the Z_S should be very much greater than Z_L. On the other hand, for 50 Hz power line frequency energy feed, value of Z_S at 50 Hz, should be very much smaller than the ohmic value of Z_L.

Digital Object Identifier 10.1109/MPEL.2022.3171644
Date of current version: xxxxxx

2329-9207/22©2022IEEE

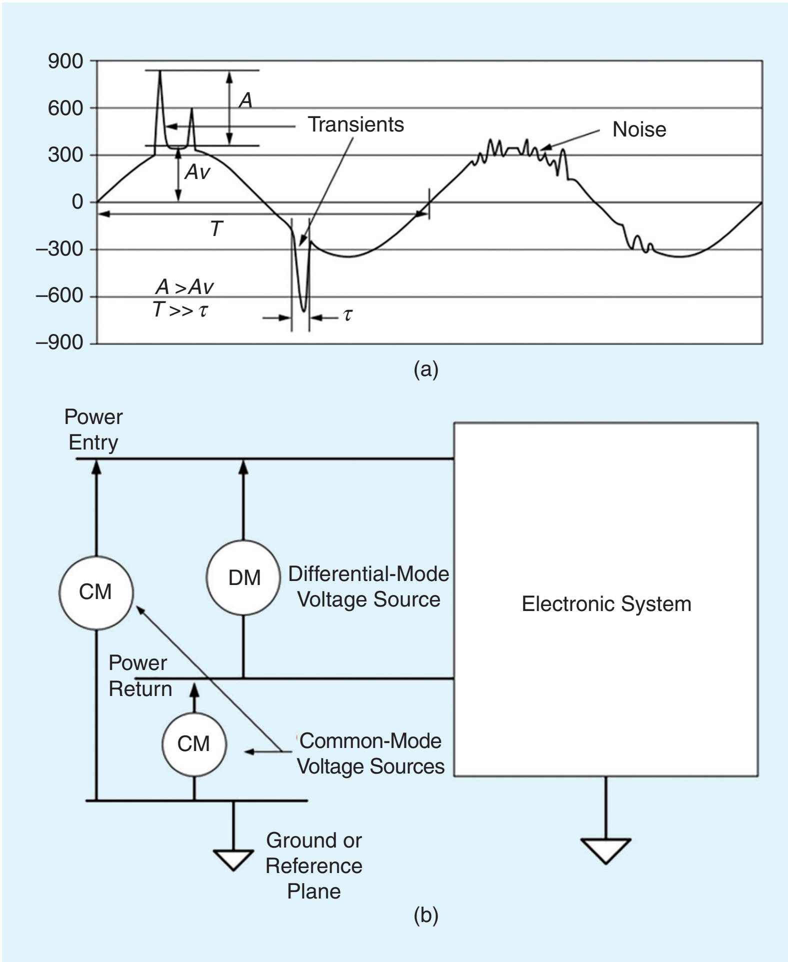

FIG 1 Transient and noise on the utility 230 V, 50 Hz power supply and the concept of differential and common mode transients entering an electronic system (a) transients and noise on utility power supply (b) common and differential mode signals.

Figure 2(b) depicts how an additional series non-linear resistance can come into play in safeguarding the load. For the frequency components of the surge, $|Z_{block}|$ should be very much higher than $|Z_L|$. Figure 2(c) shows how a non-linear shunt device can help reduce the impact of transient surge on the load, by Z_{shunt} becoming very small value due to the effect of the transient on the inserted non-linear device.

Figure 3 shows a typical case of a traditional surge protector designed to cater for both differential mode and common mode surges, where the simple concepts discussed in relation to Figure 2 are applied, using metal oxide varistors (MOV), bidirectional break-over diodes (BBD) and L-C filters combined. The MOVs and BBDs, when fired due to high transient surge voltage, they show very low shunt impedance, as depicted in Figure 2(c). Series path inductors act as high impedances at frequencies associated with the surge pulse in the order of microsecond duration, based on $2\pi fL$, where f represents the harmonic frequencies of the surge transient waveform. Shunt capacitances similarly act to show low shunt impedances at harmonic frequencies of the surge based on $1/2\pi fC$. A detailed explanation is available.

Surge Protection Standards and Practices

In most countries, the equipment connected to power lines has to be certified by nationally accredited testing laboratories. Most of these national standards are based on the international standards of the International Electrotechnical Commission (IEC). In North America the international standards of the IEC are not valid; instead, standards by the American National Standards Institute (ANSI) and the Institution of Electrical and Electronic Engineers (IEEE) are used, together with the safety standards developed by Underwriters Laboratories Inc. These standards cover the areas such as SPD specifications for different locations, SPD test procedures, and test waveforms. Table 1 lists some of these institutions and their standards in relation to SPDs [1], [3].

Locations and Categories

When a transient propagates through power lines, data lines, or other branched circuits, its energy gets dissipated in several ways. While wire resistance, flashovers, and SPDs in the surge path dissipate part of the energy, the branch circuits divide the energy to smaller quantities depending on the branch impedances and transfer these into individual branches. Due to this fact, facilities are divided into different location categories and specific protection levels are defined based on locations. Figure 4 shows IEEE C62.41 and UL 1449 defined standard location [4]–[6]. The standards classify surge protector types based on the potential impact of the transient surge, and location.

As we see from Figure 4, categories A to C are based on how far the protected equipment is from the power line entry area of the building. It shows that the closest area to power line entry point is category C and

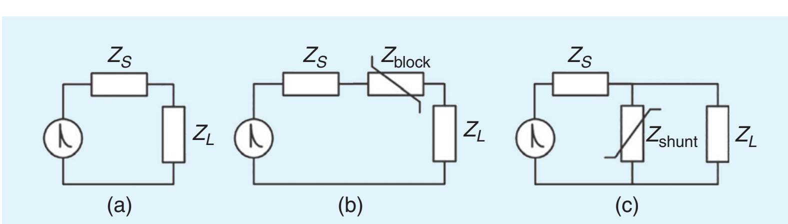

FIG 2 Voltage division principle applied to SPDs (a) basic divider formed (b) a series non-linear device helping the clamping voltage (c) shunt device action.

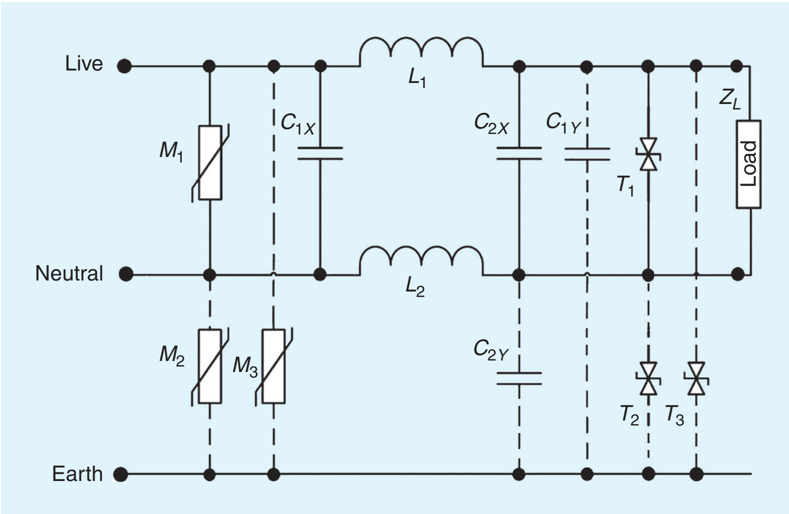

FIG 3 Typical arrangement of a commercial surge protector deigned for both common and differential mode surge absorption.

furthest areas are defined under category A. More details, and how IEEE C 62 series standard categories relate to UL 1449 types are summarised in [1].

Surge Test Waveforms

The IEC 61000-4-5 standard specifies a combination wave consisting of two waveforms, which are shown in Figure 5. The 1.2/50 µs open-circuit voltage waveform and the 8/20 µs short-circuit current waveform are shown in Figure 5(a) and 5(b) respectively. These impulse waveforms are defined by their rise times and half-amplitude duration. For example, an 8/20 µs impulse current would have an 8 µs rise time from 10% of the peak current to 90% of the peak current. The 20-µs decay time is measured between half amplitude points. Commercially available lightning surge simulators could generate these standard waveforms, where peak value of the voltage or the current is adjustable as required.

Mathematical representation of these waveforms are available in relevant standards, and Table 2 provides the details of standard test waveforms used in different location categories. Effect of external transients in 'A' location is negligible due to the protection provided by the inductance of the building wiring. Category B location is exposed to both internally created and lightning created transients and hence both ring wave and combination wave test parameters are defined. Category C has the highest exposure for lightning and utility switching transients. Combination waveform with high current and voltage, 3–10 kA and 6–20 kV waveform parameters are specified for category C locations.

Supercapacitors Capability to Absorb Transient Surges

Authors have set up a high voltage transient test laboratory with several transient surge simulators and tested several commercial families of supercapacitors to confirm that the devices themselves can withstand transient surges with peak voltages up to several kilovolts and the results are presented in [7]. This section provides an overview of the

Table 1. Test Agencies and Their Recommended Standards for Surge Protection.

Standard Agency	SPD-Related Standards	Remark
IEC	IEC 61000-4-5	Provide a model to simulate surges and then to be able to check if the equipment is able to survive them.
	IEC 60364	General rules
	IEC 61643-11	Product standards
	IEC 61643-12n	Selection and application guide
UL	UL 1449	Primary concern is safety.
	UL 1449 3rd Ed	Devoted to surge protection manufacturers, defines the parameters as well as the test procedure to qualify an SPD.
ANSI/IEEE	IEEE C62.41.1	Risk of transient over voltages to low-voltage networks.
	IEEE C62.41.2	Surge environment and types of transients.
	IEEE C62.45	Method for testing equipment against transients that are connected to the low voltage network.
	IEEE C62.62	Tests and ratings for SPDs installed on the load side of the service equipment, used to compare SPD performance.
	IEEE C62.72	Installation of SPDs in electrical power distribution equipment.
NEC	Article 280	Surge arrestor installed on wiring systems over 1000 V.
	Article 285	Selection and installation conditions of SPDs.
NEMA	LS1 Low-voltage surge protective devices	Provides specific SPD performance. This result can be used to compare actual test results of SPDs.

UL-*Underwriters Laboratory Inc.*; IEC- *International Electrotechnical Commission*; ANSI/IEEE- *American National Standard Institute/Institute of Electrical and Electronics Engineers*; NEMA-*National Electrical Manufacturers Association.*

theoretical foundations related to these encouraging test results which led to the development of the supercapacitor assisted surge absorber (SCASA) technique [8], [9], which culminated multiple international patents.

Supercapacitors can be simply summarised as a device family where you could achieve over one million times larger capacitance for the same canister size as electrolytic or film capacitors. New commercial devices come in three different variations, namely (i) symmetrical electrical double layer capacitors (ii) hybrid devices where one electrode is similar to electrodes used in Li rechargeable batteries, and (iii) pseudo-capacitance based [9]. These commercial single cell devices are in the range of 1 F to over 70,000 F and in the SCASA technique, symmetrical double layer capacitances in the range of 1 to 100 F are used, given their very low cost [10].

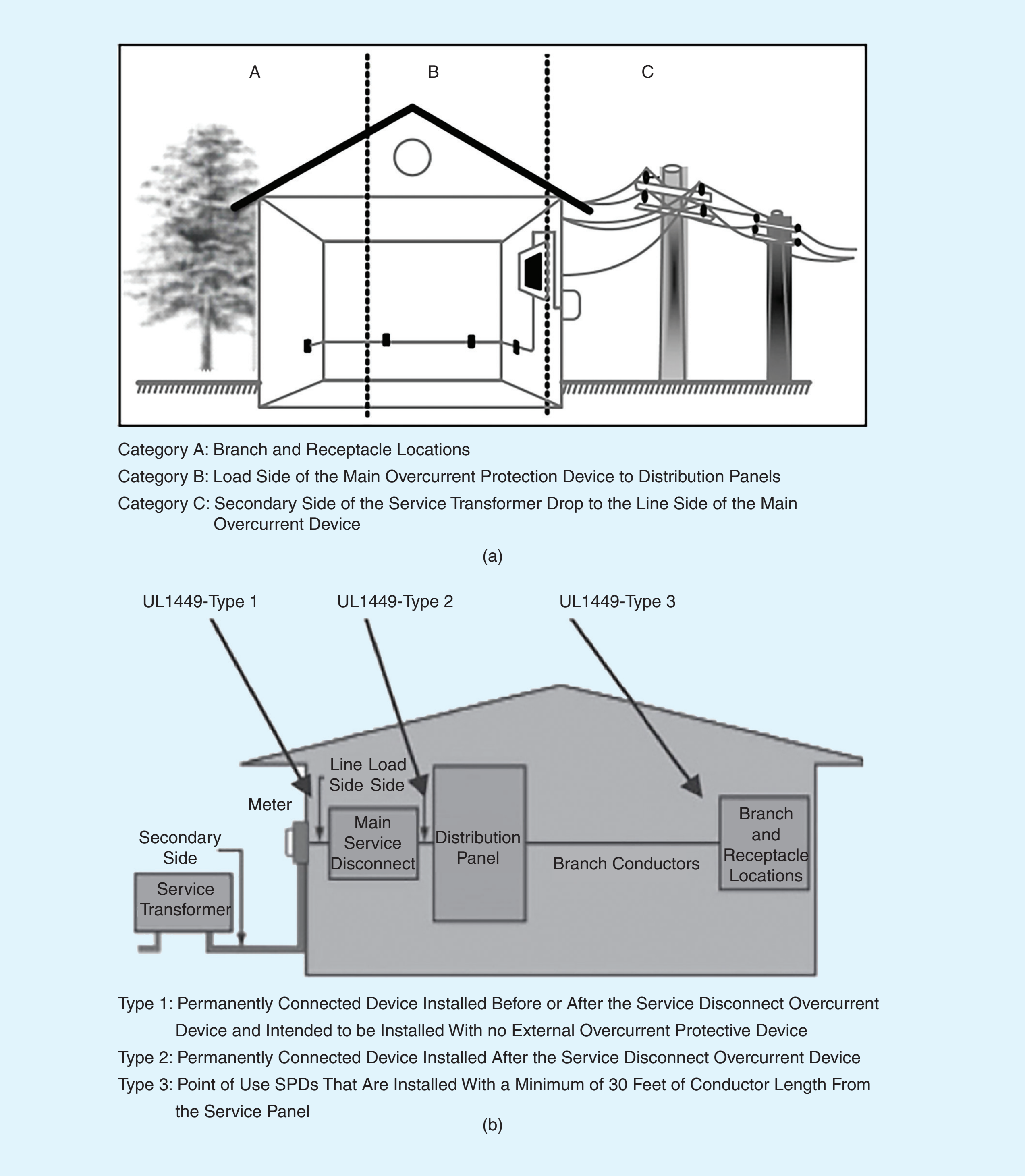

FIG 4 **Locations and categories of surge protectors in a building and associated standards.**

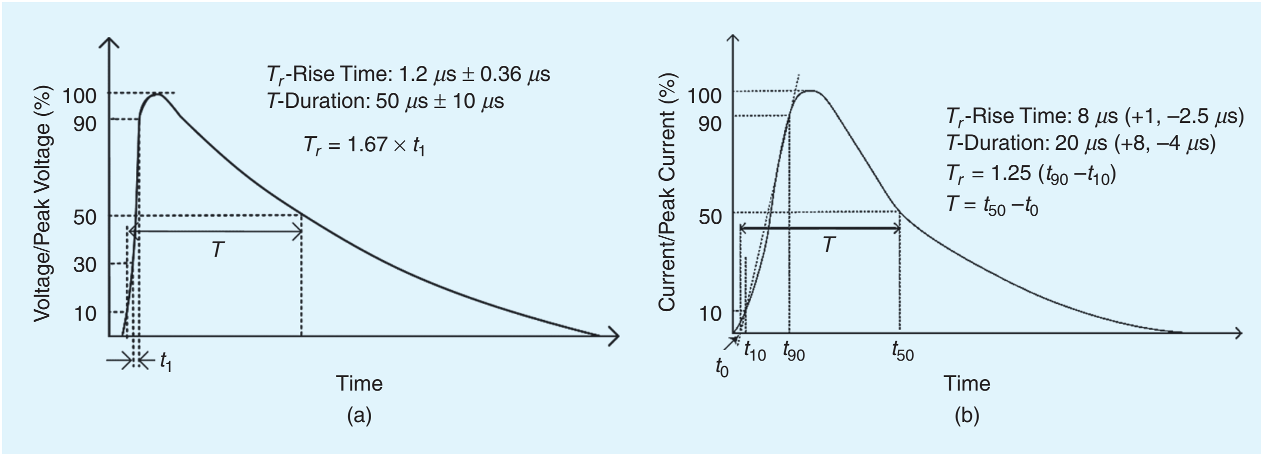

FIG 5 Standard test waveforms defined by IEC 61000-4-5 (Combination wave) (a) open circuit voltage (b) short-circuit current.

Table 2: IEEE C62-41 Location Based Current/Voltage Waveforms.

			0.5 μs x 100 kHz Ring Wave		1.2 x 5 μs (V) 8 x 20 μs (A), Combination Wave	
Category	Level of Exposure	Voltage (kV)	Current (A)	Energy (J)	Current (kA)	Energy (J)
A1	Low	2	70	0.63	-	-
A2	Medium	3	130	2.34	-	-
A3	High	6	200	5.43	-	-
B1	Low	2	170	1.53	1	9
B2	Medium	4	330	5.94	2	36
B3	High	6	500	13.5	3	81
C1	Low	6	-		3	81
C2	Medium	10	-		5	225
C3	High	20	-		10	900

Given the very large capacitance of a SC, and most types with a very low ESR in the order of 1 mΩ to over 100 mΩ, a SC in a practical circuit creates a large time constant circuit. For example, a 1 μF electrolytic capacitor in a resistive circuit with a total loop resistance of 1 Ω creates a circuit with a time constant of 1 μs. If this RC circuit is fed by a dc voltage source after about 5 μs it will reach the dc supply's voltage. This means that if the dc rail is a step voltage source of over 5 μs duration, the capacitor could reach its maximum voltage, while storing 0.5 CV^2 Joules. If the capacitor was starting with a zero charge, the resistive parts of the loop will dissipate the same amount of energy.

However, if the electrolytic capacitor is replaced by a SC of 1 F, the circuit will take over 5 seconds to charge the capacitor fully, if the dc source is steady. Now if the SC based RC circuit is fed by a step dc source lasting only 5 μs, capacitor charge will be pretty low, and the energy stored in the SC will be also very low. During this time the loop resistance wastes the energy based on the squared value instantaneous loop current and the total loop resistance. The energy stored in capacitor during the step voltage will be every much lower than the energy dissipated in the cumulative resistance of the loop.

Based on the above qualitative explanation, we can analyse the case of an RC circuit based on a SC subjected to a high voltage transient of limited duration. Figure 6(a) depicts this case with a capacitor of value C, and its ESR of value R and the total parasitic loop resistance of R_p. If a step dc voltage of duration of T is given as vin, applying Kirchhoff's voltage law to Figure 6(a),

$$v_{\text{in}} = iR + iR_p + \frac{1}{C}\int_0^t i\,dt \qquad (1)$$

$$i(t{:}0<t<T) = \frac{V_{\max}}{R_T}e^{-t/CR_T} \qquad (2)$$

$$v_c(t{:}0<t<T) = V_{\max}\left(1 - e^{-t/CR_T}\right) \qquad (3)$$

where, $R_T = R + R_P$ and $V_{\max}$ is the pulse voltage as depicted in Fig 6(b).

Assuming that the capacitor is initially fully discharged, energy dissipated in the capacitor ESR, E_R, is given by,

$$E_R = \int_0^T i^2 R\,dt = \frac{CR}{2R_T}V_{\max}^2\left(1 - e^{-2T/CR_T}\right) \qquad (5)$$

At time T, the capacitor has accumulated an energy, E_c, of

$$E_C = \frac{1}{2}Cv_c^2 \qquad (6)$$

Where $v_c = V_{\max}\left(1 - e^{-t/CR_T}\right)$,

Figure 6(c) shows the development of current in the loop and voltage across the capacitor for a case of pulse duration of 50 μs, and a maximum current from a transient surge source of 3000 A (such as a lightning surge simulator, discussed later). Figure 7 depicts the effect of above analysis

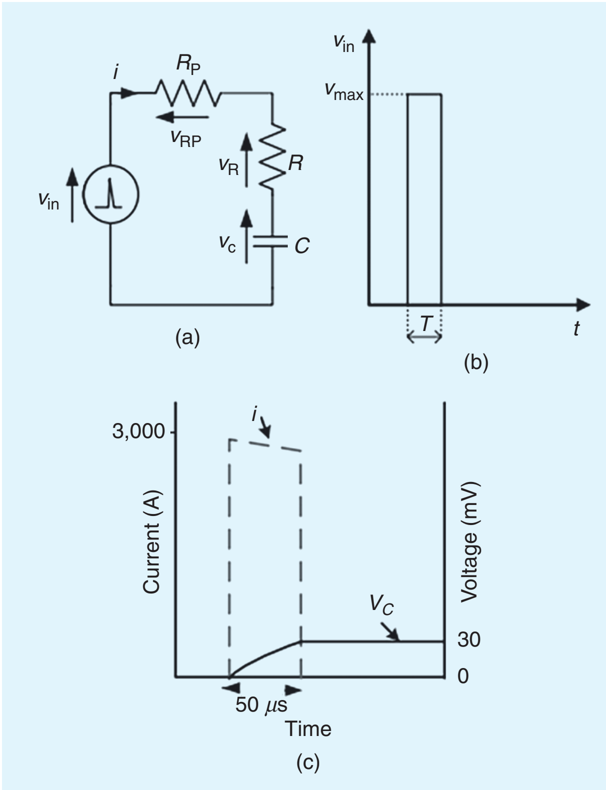

FIG 6 Applying a short duration pulse on a supercapacitor (a) RC circuit fed by the transient surge source of short duration (b) step voltage waveform of duration T (c) resulting current and voltage waveform for the SC.

in Equations (1) to (5) when the surge is equivalent to a 6 kV step dc source of duration 50 µs. While the lower right hand side of Figure 7 shows the cases of three different SCs of values 1 F, 5 F and 100 F, upper left hand side of the Figure shows the cases with the supercapacitors replaced by 100 µF, 470 µF and 1500 µF.

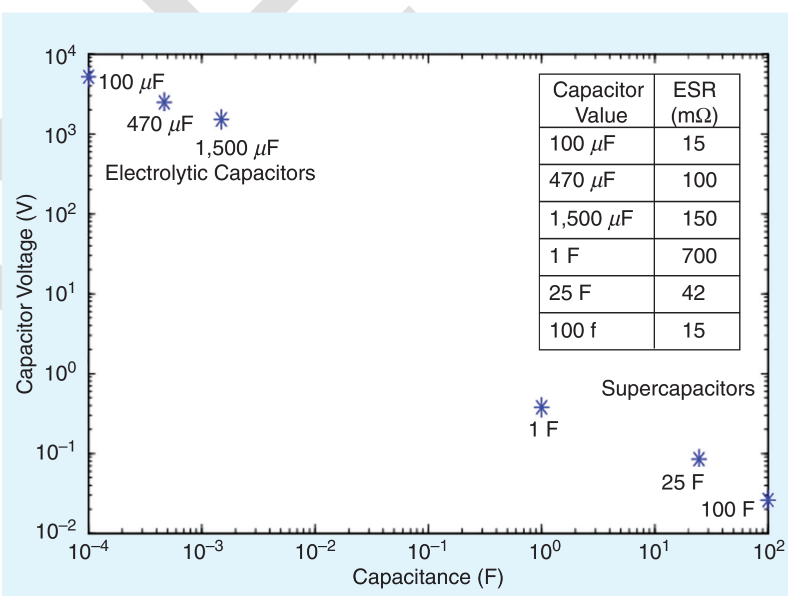

FIG 7 The voltage build up on different capacitors for a 6 kV, 50 µs single pulse. Capacitors chosen are 100, 470, and 1500 µF electrolytic capacitors, and 1, 25, and 100 F SCs.

What Figure 7 shows in summary is the case that supercapacitors in an RC loop fed by a HV transient pulse does not damage or destroy SCs, compared to an electrolytic capacitor set of similar can size (and price), since the SCs do not charge beyond their rated dc voltage. More details are available in [1], [10]. As Figure 7 indicates, while supercapacitors maintain the voltage within their dc ratings, in electrolytic capacitors, they get charged up to several 1000 volts.

In Figure 8 we see a different, but a more useful interpretation of this concept.

In a real world situation, charging loop will have the capacitor which offers a farads order supercapacitor, with a finite, but small ESR (larger the SC smaller the ESR) together with its parasitic loop resistance, where theory related to the Figure 7 still applies. Under this situation, energy dissipated in the SC loop is of importance, since it can create heat within the device (due to the effect of the ESR), and push the capacitor beyond its safe temp range. It can be shown that [12] energy dissipated in ESR of the SC as a ratio of energy absorbed by the SC is given by,

$$\frac{E_R}{E_C} = \frac{\frac{1}{2}\frac{CR}{R_T}V_{\max}^2\left(1-e^{-2T/CR_T}\right)}{\frac{1}{2}CV_{\max}^2\left(1-e^{-T/CR_T}\right)^2} \tag{6}$$

$$= \frac{R}{R_T}\frac{\left(1+e^{-T/CR_T}\right)}{\left(1-e^{-T/CR_T}\right)} \tag{7}$$

These mathematical relationships in summary indicates the case of a supercapacitor's capability to dissipate short-term surge energy in path resistances and/or ESR of the device, compared to an electrolytic capacitor of a similar can size. Based on the same theory, Figure 9 depicts what happens to the voltage across the capacitor, with repeated surges applied from a lightning surge simulator such as Noiseken LSS 6230. It is important to note that the vertical axis is in the units of millivolts, and hence do not tend to exceed the rated dc voltage of the device.

In summary this discussion provides the background to use a SC based sub-circuit to develop a more effective SPD.

Problems with Supercapacitors as Shunt Devices

Referring to Figure 3, in a surge protector application, critical load is safeguarded by the action of shunt devices such as the MOVs and the BBDs. Given these conditions of the MOV/BBD are kept in parallel to the ac utility mains line, they should

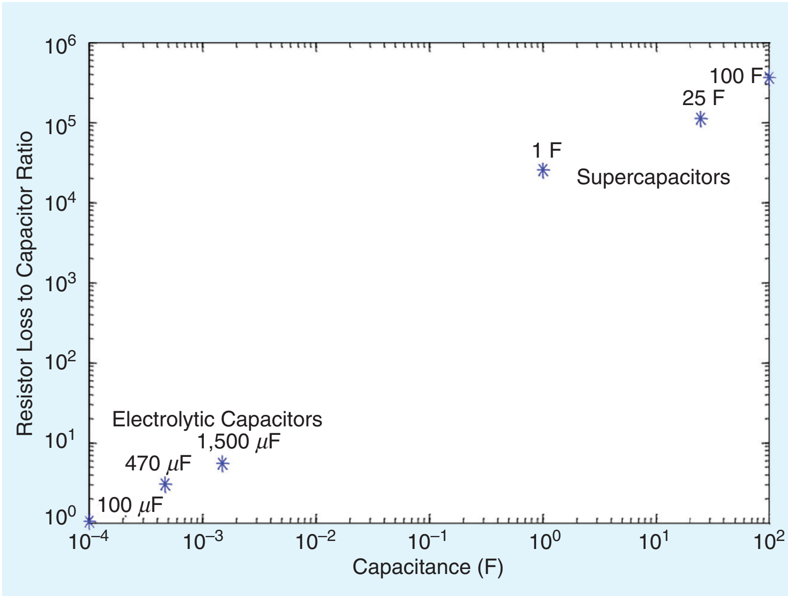

FIG 8 Comparison of energy lost and stored for electrolytic capacitors and SCs subjected to a 6 kV, 50 μs pulse. Capacitors chosen are 100, 470, and 1500 μF electrolytic capacitors, and 1, 25, and 100 F SCs with 15, 100, 150, 700, 42, and 15 mΩ ESR, respectively.

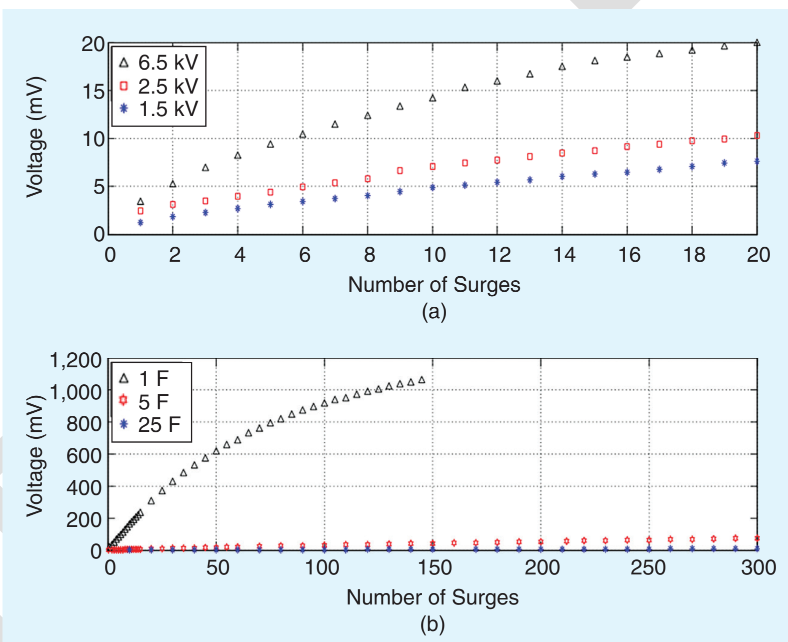

FIG 9 Applying consecutive surges to supercapacitor. (a) different surge voltages to a 5 F capacitor; (b) 6 kV peak surges to different capacitors.

have a voltage rating that under nominal line voltage and its worst case (RMS voltage) variation, they do not fire into conduction, and they can withstand the instantaneous line voltage.

Compared to this essential requirement, since supercapacitors have very low voltage dc ratings in the range of 2 to 4 V (for single cell cases), they cannot directly replace MOVs or BBDs in a surge protector. Also, at 50 or 60 Hz of power line frequency, if you place a SC between live and the neutral of the ac mains, it will show a very small shunting impedance determined by $1/2\pi fC$ which will in turn create an effective short circuit across the line and the neutral. For example, 1 F SC will show an impedance of approximately 3.1 mΩ at 50 Hz. However, a 1 μF film capacitor, will show a shunt impedance of 3.1 kΩ. This simply argues about the difficulty of using a SC based shunt sub-circuit to absorb transient surge voltages superimposed on the power line.

Supercapacitor Assisted Surge Absorber Concept

Power electronics research group at the University of Waikato, launched a PhD thesis completed by the first author [10]–[14], based on the preliminary investigations which lead to the first patent [8]. As per detailed research published in [12]–[16], a uniquely new circuit topology as per Figure 10(d) was successfully developed by the team at Waikato. This was based on a step by step analysis of Figures 10(a) to 10(c). Following paragraphs provide a summary of the applicable theoretical concepts, and the associated design and development process.

Based on the summaries provided in the above sections (Supercapacitors Capability to Absorb Transient Surges and Problems with Supercapacitors as Shunt Devices), while a SC and a resistor based circuit can be used to dissipate transient energies associated with high voltage transients superimposed on the power line, the low voltage dc rating and the extra-low ac impedance (at line frequency) is a major issue to replace a MOV or BBD directly. Another useful information is the joules order energy absorption capability of the SCs based on $0.5\,CV^2$. For example, a 5 F SC with a dc rating of 2.7 V could safely-store 18.2 Joules. A 100 F SC with same dc voltage rating could store 364 Joules. A typical class A/B type SPD is expected to handle few joules to over 100 J surge energy, based on a combination wave or a current waveform generated by a lightning surge simulator.

As per Figure 10(a), a simple inductor and a MOV type surge absorber can be combined to provide protection against transient surge voltages of microsecond durations. When the transient surge voltage exceeds the firing voltage of the surge absorber (MOV or the BBD) parallel to the protected load, a current is induced in the input loop, and

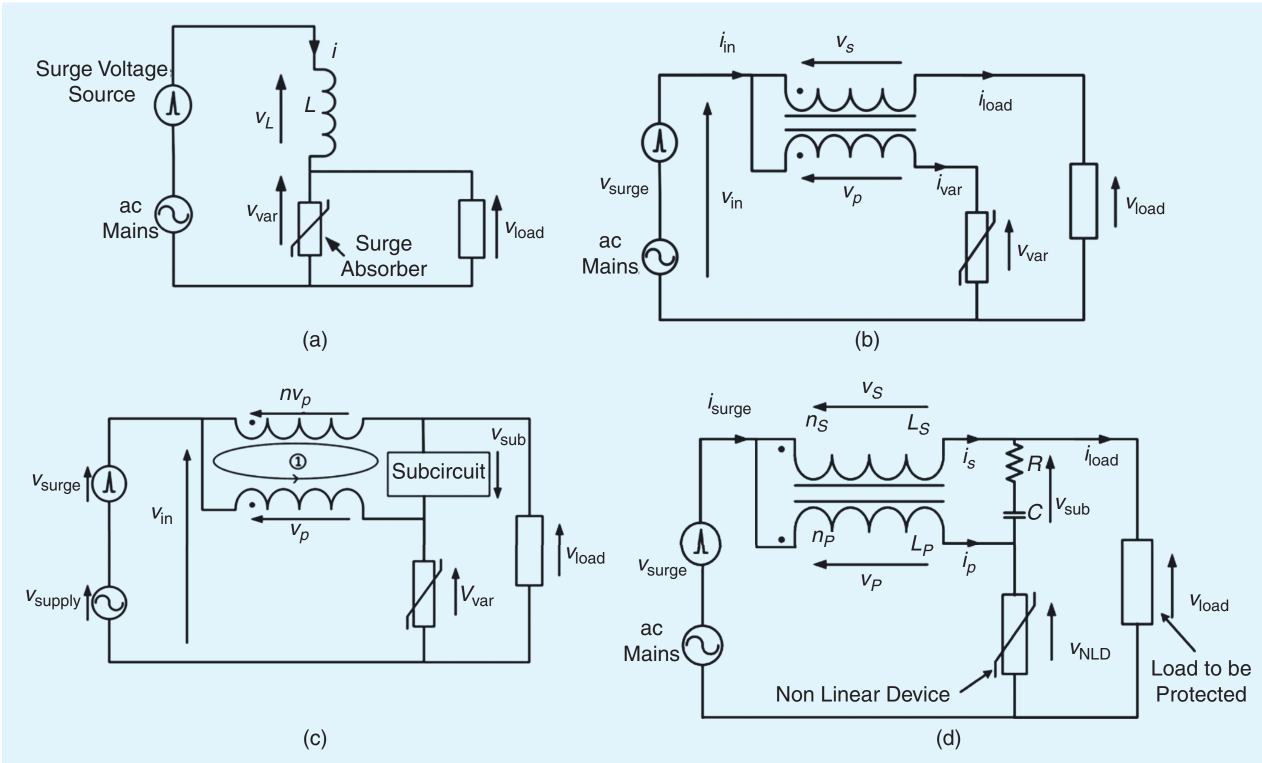

FIG 10 Conceptual development of the SCASA protector (a) a series inductor with a high voltage clamping device (b) use of a coupled inductor instead of the case in part (a) (c) a SC based sub-circuit to form a closed loop with the primary and the secondary windings (d) commercially produced version with two MOVs and one low-cost SC.

inductor develops a voltage of $L\,di/dt$ maintaining the following relationship,

$$V_{in} = V_{var} + L\frac{di}{dt} \tag{8}$$

where V_{in} is the instantaneous input voltage due to superimposed surge, and V_{var} is the instantaneous voltage across the MOV which will be the same as the instantaneous voltage at the load. Under normal 50 or 60 Hz only line voltage, MOV is under off condition and with a very small inductor, load will see the rms ac voltage approximately. Once the MOV enters into conduction, until the transient surge disappears, V_{var} will be approximately equal to the clamping voltage of the MOV.

Figure 10(b) depicts how we could extend this into a coupled inductor wound on a suitable magnetic core, to perform the function of a loosely coupled transformer where primary winding is in series with the MOV and the secondary winding in series with the protected load, while input ends of both windings are connected to the input ac mains. This two winding loosely coupled magnetic component (with coupling coefficient $k = 0.74$) is purposely selected so that it creates a high leakage inductance to attenuate the surge voltage. By the inductor placement and the polarity arrangement of the coupled inductor, it is possible to:

- Trigger the coupled inductor to carry a primary current when the varistor (MOV) fires at the event of transient voltage superimposed at the input power line.

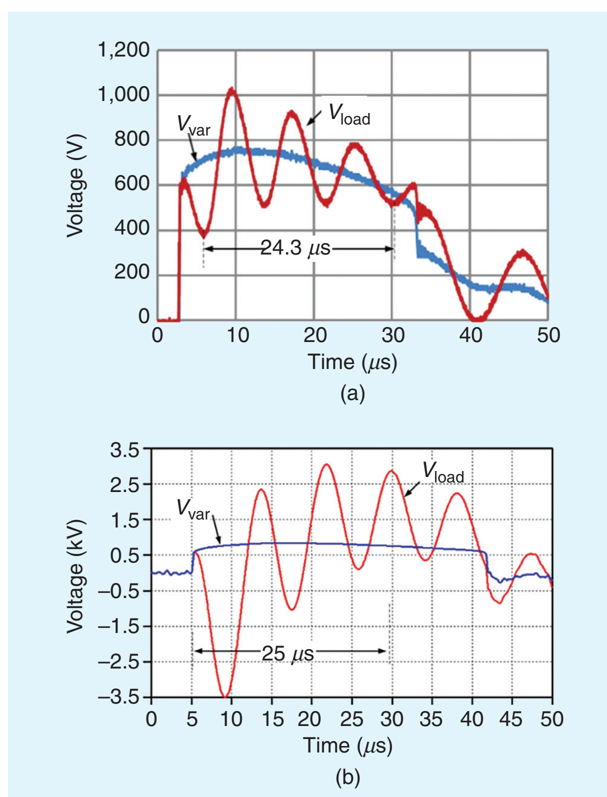

FIG 11 Effect of sub-circuit capacitor on load voltage during the surge (a) experimental results for 47 nF capacitor (b) simulation results for 47 nF capacitor.

- Reduce the load voltage (transient related) during the high voltage transient surge
- Store part of the transient surge energy in the inductive elements of the coupled inductor (where self and magnetizing inductances of the non- ideal transformer comes into play)

To analyze the coupled inductor circuit, assume the perfect coupling to describe the transformer turns ratio, which allows the desired operation. SC is connected between the load side ends of the two coils so that it helps creating a closed loop via the SC for absorbing part of the surge energy. Input side end of the two coils are connected together and the common point is attached to the live wire of the input power source. Common point of the SC and the secondary coil terminal forms the output node, which is connected to the critical load.

From varistor current, i_{var} and load current branches in Figure 10(b).

$$v_{\text{in}} = v_{\text{var}} + v_p = v_s + v_{\text{load}} \tag{9}$$

If the transformer has n_p primary turns and n_s secondary turns, turns ratio, $n = n_s/n_p$, then $v_s = nv_p$. Hence the load voltage can be expressed as:

$$v_{\text{load}} = v_{\text{var}} + v_p - nv_p = v_{\text{var}} - (n-1)v_p \tag{10}$$

Because the design should lower the voltage seen by the load to a voltage less than the varistor clamping voltage.

$$v_{\text{load}} < v_{\text{var}} \Longrightarrow (n-1)v_p > 0 \tag{11}$$

Because $v_p > 0$ for a positive transient,

$$n-1>0 \Longrightarrow n>1 \tag{12}$$

To provide a complete analysis with design calculations leading to a testable prototype of the SCASA is beyond the scope of this paper. These details are available in [1, 12-16]. A summary useful for a designer is given below, based on the preliminary prototypes build and the first commercial product developed which will be discussed later.

i. The coupled inductor's secondary should work as a step-up winding to lower the transient related voltage appearing at the load.
ii. Technique provides the unique advantage of transient related load voltage will be less than the varistor's clamping voltage.
iii. There is a limit to increasing the turns ratio, to prevent transient load voltage reaching a negative value
iv. Coupled inductor's windings should not create any excessive series inductance into the load loop at the 50 Hz line frequency.
v. Supercapacitor sub-circuit shown in Figure 10(c) assists the dissipation of the surge energy by forming a closed loop due to SC path, without any unwanted ringing waveforms related to the transient surge energy.

For readers to gain more insight into this technique in terms of theoretical concepts, Ref [10] is suggested.

Selection of Supercapacitor and the Magnetic Core

To achieve a practically useful SPD based on the SCASA technique, correctly selecting the supercapacitor and the core for the coupled inductor are the most important key design decisions. At the early development stage of the technique, research team considered using a film capacitor in the order of tens of nano-Farads, instead of a SC. This was to justify the value of using a small supercapacitor, to assist the absorption and dissipation of the transient surge energy, so that SPD's ability to survive without major degradation of the MOVs, when subjected to repeated surges under UL 1449- 3rd Edition tests.

Figure 11 depicts the case where the SC is replaced by a similar can size 47 nF capacitor. Figure 11(a) shows the experimental results and Figure 11(b) depicts the simulation results. In both cases, it can be observed that the voltage across the load creates a ringing effect with an approximate frequency around 120 to 125 kHz.

Figure 12 shows the transient performance of the actual SCASA circuit based on a 1F SC and a resistor subjected to C62.41 standard based surges, where peak voltages at 1 kV and 6.6 kV were supplied from a lightning surge simulator. In both experimental and simulated results, it can be observed that the transient related load voltage does not create any ringing effects, as in the case of using film capacitors in the sub-circuit.

This discussion indicates clearly that the supercapacitor assisted new topology helps in the surge absorption, based on a coupled inductor approach at the input end. In developing this new topology, the coupled inductor acts as a loosely coupled transformer, when the MOV enters into conducting stage. Design of this coupled inductor was based on a permeance (inductance per square turns) based approach, as detailed in [10], [16]–[19]. Without a detailed discussion, at the first stage of research and development, the research team had a concluding result that powdered alloys work effectively in the SCASA design while ferrite cores were not effective. Due to high permeability/permeance of ferrites (Figure 13), they cannot be used in their original form for SCASA design. But, in the gapped form (single-gapped or double-gapped), ferrites perform satisfactorily. More investigations about air-gapped ferrites and other suitable magnetic materials are found in [20].

In summary, out of various commercially available magnetic materials, the optimum range of core permeability was found to lie within $\mu_r = 26 - 60$, and the wound magnetic component should be such that the magnetic coupling coefficient lies within $0.56 < k < 0.74$. Moreover, as X Flux toroid shows ~60% better saturation flux capacity (16,000 gauss) compared Kool μu (10,500 gauss) as illustrated by Figure 13, functional limitations of SCASA circuit at high-magnitude surge currents can be prevented. Since a detailed discussion about the magnetic component selection of SCASA is beyond the scope of this paper, we highlight essential properties of various magnetic materials used for prototype design in Figure 13.

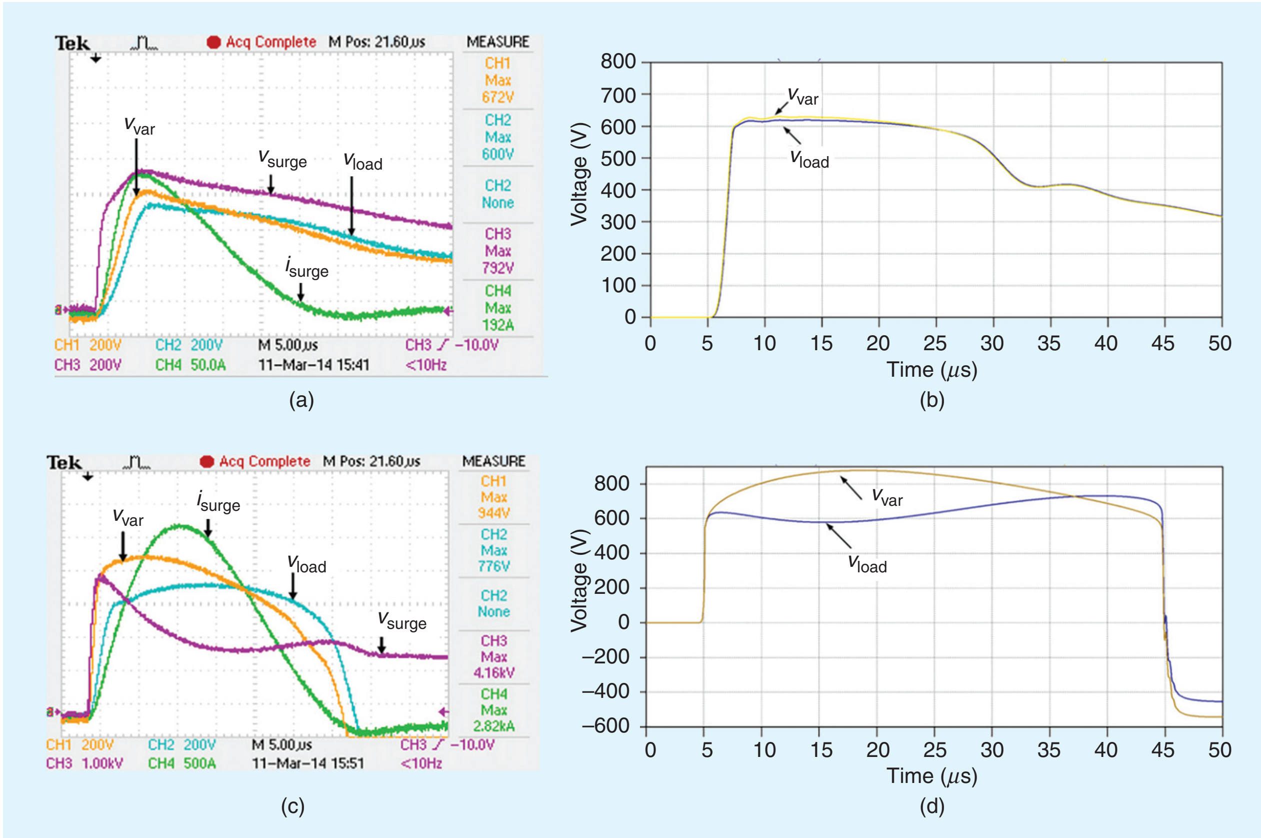

FIG 12 Experimental and simulation results for different surge voltage inputs on a SCASA prototype (a) Actual oscillogram for a 1 kV surge (b) simulated results for a 1 kV surge (c) Actual oscillogram for a 6.6 kV surge (d) simulated results for a 6.6 kV surge.

Magnetic Core Type	Kool Mu (Present SCASA)	High Flux	X Flux	W Ferrite
				
Permeability (μ_r)	60	60	26	10,000
Permeance (Λ_m) (nH/turns^2)	61	61	28	13,400
Saturation Flux Density ($\vec{B}_{max}$) (Gauss)	10,500	15,000	16,000	3,900

FIG 13 Comparison of magnetic properties of different powdered-iron and ferrite based alloys used in SCASA prototype design.

Development of a Commercial Prototype, and testing under UL 1449 Standard-3rd Edition

SCASA technique is a unique new way to design a high endurance capability SPD, using a supercapacitor sub-circuit to improve its ability to withstand repeated surges, with minimal or no degradation to its components. In a typical MOV dominated traditional surge protector, with repeated transient surges absorbed by the internal components such as the MOVs, the effective performance degrades over time. UL 1449 3rd Edition specifies the requirements of a commercial SPD, subjected to repeated surges, and the respective abilities of internal components of a SPD to survive without any disastrous failures. SCASA technique summarised in Section on "Supercapacitor Assisted Surge Absorber Concept", and its design calculations summarised in [1], [12] led to the design of a commercial version, as shown in Figure 14.

Product shown in Figure 14(a) is aimed at protecting indoor appliances such as LCD TVs, computers and high-fidelity systems and therefore it is designed to safeguard against differential mode transients. As shown in Figure 14(b), the overall circuit carries two MOVs, one powdered alloy based coupled inductor and a supercapacitor-resistor based sub-circuit. For readers interested in the design calculations, Ref [10.] is recommended. A powdered core from Magnetics, USA with a relative permeability of 60 and a permeance value of around 81 nH/Turns^2 was used, since most ferrites with large relative permeability were not useful [16]. While maintaining the confidentiality of commercial details, the overall implementation achieved the following essentials required in a commercial SPD adhering to the UL 1449 3rd Ed.

- Showing very low series impedance at 50/60 Hz to allow power flow to the load side
- At the occurrence of a transient, first MOV (Var_1) in Fig 14(b) fires and creates a activation of the coupled inductor to develop a secondary voltage opposing the imposed surge voltage
- SC sub-circuit absorbs part of the transient surge energy due to the closed loop formed by the two windings creating opposite voltages, where the difference creates a loop current via the SC sub-circuit attempting the charge the SC, while dissipating part of the surge energy in the cumulative resistance of the inductive loop.
- Energy of the transient surge is shared among (i) Var_1, loop inductances, and the supercapacitor sub-circuit. Stored energies in the SC and the inductive elements are dissipated with some delays.
- In case the remaining (transient related) output voltage is over the firing point of the Var_2, it fires and reduces the impact on the critical load protected by the SPD.
- Over 100 repetitions of 6.6 kV, 3 kA surges were applied as per UL 1449 guidelines and no deterioration of the components were observed.
- The most unique property is the transient related peak appearing at the load is always less than the MOV's clamping voltage.

Table 3 provides a comparison of number of components for differential mode section in two commercial version (sold in New Zealand) and the number of components in the SCASA based commercial product. This clearly shows, that SCASA uses much lower number of components, than a high-end commercial SPD.

Table 4 depicts another key performance related characteristic of SCASA technique. By the introduction of the coupled inductor into the SCASA technique, with a SC based sub-circuit, it increases the lifetime of the varistors used inside the circuit significantly. Table 4 compares the cases

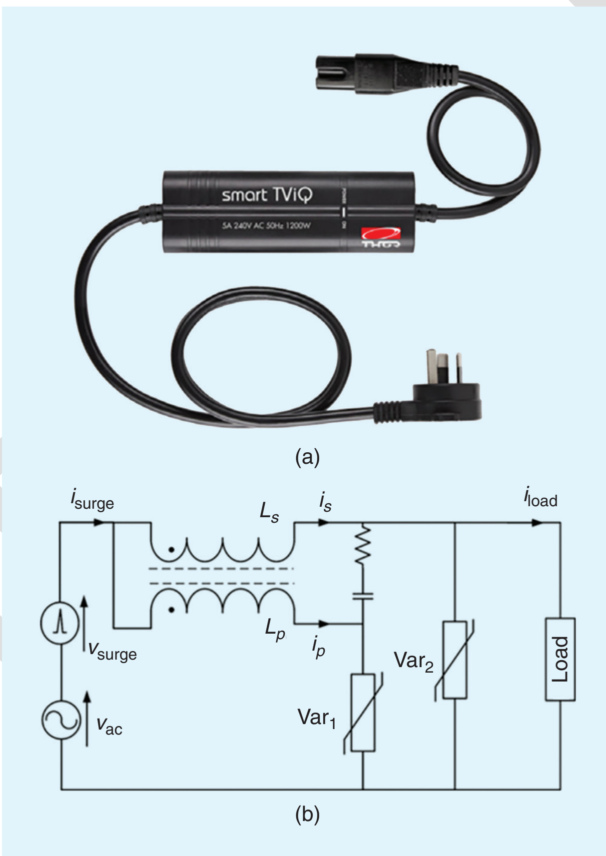

FIG 14 The commercial product and essentials of its internal circuit (a) Smart TVIQ[2] which was launched in the Australian market based on the SCASA technique [Courtesy of Thor Technologies, Perth, Australia] (b) SCASA technique with an additional second varistor for added safety against repeated surges.

Table 3 Component Count Comparison for Differential Mode Section in Commercial SPDs and SCASA based SPD.

Component Type	High End	Low End	SCASA
MOVs	4	1	2
Inductors	2	0	1
X-type capacitors	5	1	0
Supercapacitors	0	0	1

Table 4. Destructive Varistor Tests on the Commercial Product.

Varistor (Ref:figure 14(b))	Rated energy (J) (Based on 10/1000 µs test waveform)	Rated AC Voltage (V)	Test result
Varistor 1 (431KD14)	*66*	*275*	*Sample 1–Failed after 7 surges of 6 kV peak*
			Sample 2–Failed after 10 surges of 6 kV peak
Varistor 2 (431KD10)	*132*	*275*	*Sample 1–Failed after 34 surges of 6 kV peak*
			Sample 2–Failed after 27 surges of 6 kV peak

of failures of MOVs used as Varistor 1 and Varistor 2 [Figure 14 (b)] and the required number of repeated surges to destroy them. For 6 kV surges both versions (when individually tested) failed even before 40 repeats, whereas overall SCASA system could withstand much above 100 repeated surges, without any degradation of the components.

Appendix B1 in Ref [1] is a summary of commercial test report on Smart TVIQ2 product subjected to UL 1449 3rd Edition recommendation. It also gives an overview of how to interpret test data created by the test procedure, utilizing a commercial lightning surge simulator (LSS) of the type Noiseken LSS 6230 and Tektronix TPS 2014 oscilloscope.

Figure 15 depicts the measured performance of the SCASA implementation, where Figure 15(a) compares its performance with two common commercial products and Figure 15(b) depicts the unique property of load seeing a lower transient related peak voltage than the clamping voltage of the varistors used.

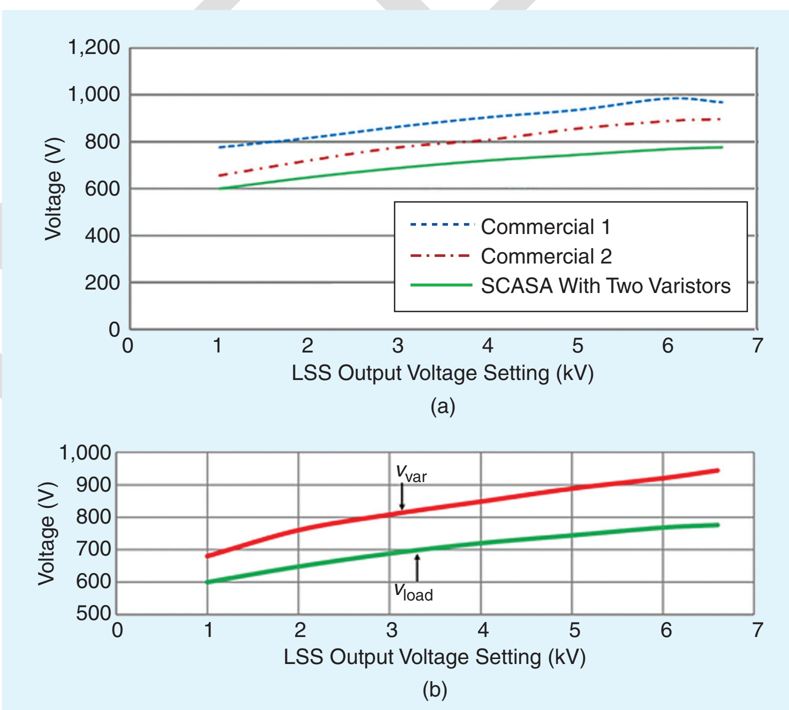

FIG 15 Performance of SCASA technique (a) comparison with traditional SPDs (b) lower load peak voltage than the varistor voltage.

Ongoing Developments

SCASA's commercial success has led us to develop the basic technique further to absorb high transient joules and also to have significant surge-repeat-endurance. One area where significant ongoing research is in the selection of magnetic cores including the gapped ferrite cores of high relative permeability, with lower costs than powdered alloys. The other area will be the advanced versions of SCASA topology based on complex core combinations. References [17], [18] provide our early results, in ongoing Ph.D projects.

Conclusion

Supercapacitor assisted surge absorber (SCASA) technique is a new technique useful for surge protectors where a SC based sub-circuit is effectively combined with traditional surge absorber devices such as MOVs. This work proves the capability of SC based long time constants in surge absorbers, as a unique new family of surge protectors adhering to UL 1449 3rd Ed standard. A unique property of the SCASA technique is to achieve a lower transient related peak voltage at the load, compared to the Varistor's clamping voltage in a commonly used SPD techniques. With repeated surge applications, as per UL 1449, the MOVs in SCASA protectors do not deteriorate with the applied number of surges. Proper selection of a magnetic core is key requirement for the successful implementation in a commercial SPD.

About the Authors

Jayathu Fernando holds B.Sc and M.Sc degrees from University of Colombo and University of Moratuwa in Sri Lanka. He completed his Ph.D at the University of Waikato in 2016, (UoW)working on the supercapacitor assisted surge absorber technique. After completing a post doctoral assignment at UoW, he joined APL Ltd. (New Zealand) as an electronic product development engineer. His industrial research interest is embedded products and power electronics.

Nihal Kularatna is research-active in supercapacitor applications and power electronics. He has authored ten reference books and research monographs, and contributed over 170 publications. He won the Post Graduate Research Supervision Excellence Award (2021) from University of

Waikato, where he is employed as an associate professor. He won the NZ Engineering Innovator of the Year 2013 award for developing his SCA techniques. He was conferred a DSc degree in 2015. Prior to moving to academia in New Zealand, he was the CEO of Arthur C Clarke Institute in Sri Lanka.

Shanima Silva received B.Eng. (Hons.) (2012) in digital communications and electronics and M.Sc.(2014) in embedded intelligent systems from University of Hertfordshire, UK, and is currently pursuing Ph.D degree in electronics at the University of Waikato, New Zealand. Currently, he is working as a senior automation engineer at Automate-X, Papakura, Auckland. New Zealand. He has also previously worked as an electrical engineer at Caterpillar in Sri Lanka. His research interests include supercapacitor assisted techniques and harmonic control in the linear ac regulator technique. He is a member of IET and IEEE.

Sadeeshvara Silva Thotabaddadurage holds a Ph.D in electronic engineering from the University of Waikato, New Zealand (2021) and a B.Sc. (Hons. -1st class) from University of Sri Jayewardenepura, Sri Lanka (2014). Soon after his doctoral study, he joined Electric Power Engineering Centre, University of Canterbury, New Zealand as a research engineer. He acts as a reviewer for IEEE Transactions on Industrial Electronics, IET Power Electronics and for IEEE conferences such as APEC, IECON, and TENCON. He is also a Member of Engineering NZ, IEEE and IET. He is passionate in research on power quality & surge protection, supercapacitor applications, transformer theory & design, frequency domain modelling and magnetics.

References

[1] N. Kularatna, A. Steyn-Ross, J. Fernando, and S. James, *Design of Transient Protection Systems: Including Supercapacitor Based Design Approaches for Surge Protectors*. New York, NY, USA: Elsevier, 2018, p. 284.

[2] "Surging ideas: TVS diode," Semtech International, Application Note AN96-07, 2002.

[3] *Technical Catalogue*, CITEL, 9th ed., 2013, p. 131.

[4] "Transient voltage surge suppressors," Underwriters Lab., Northbrook, IL, 2014.

[5] *IEEE Draft Recommended Practice on Characterization of Surges in Low-Voltage (1000 V and Less) AC Power Circuits—Corrigendum 1*, IEEE PC62.41.2-2002/Cor 1/D2, 2012, p. 110.

[6] *IEEE Recommended Practice on Surge Testing for Equipment Connected to Low-Voltage (1000 V and Less) AC Power Circuits*, IEEE Standard C62.45-2002 (Revision of IEEE Standard C62.45-1992), 2003, pp. 1–85.

[7] N. Kularatna, J. Fernando, A. Pandey, and S. James, "Surge capability testing of supercapacitor families using a lightning surge simulator," *IEEE Trans. Ind. Electron.*, vol. 58, no. 10, Oct. 2011, pp. 4942–4949, doi: 10.1109/TIE.2011.2109338.

[8] N. Kularatna and L. Jayathu Fernando, *Power and Telecommunication Surge Protection Apparatus*, NZ Patent-604332, Mar. 21, 2014.

[9] N. Kularatna and D. Jayananda, "Supercapacitor based long time constant circuits: A unique design opportunity for new power electronic circuit topologies," *IEEE Ind. Electron. Mag.*, vol. 14, no. 2, Jun. 2020, pp. 40–56, doi: 10.1109/MIE.2019.2959199.

[10] J. Fernando, "SCASA and supercapacitor surge modelling," Ph.D. thesis, Univ. of Waikato, 2016.

[11] J. Fernando and N. Kularatna, "A supercapacitor-based enhancement for standalone surge protector circuits," in *Proc. ISIE-2013 Conf.*, Taipei, Taiwan, Jun. 2013, pp. 1–6.

[12] J. Fernando, N. Kularatna, H. Round, and S. Talele, "Implementation of the supercapacitor-assisted surge absorber (SCASA) technique in a practical surge protector," in *Proc. IEEE-IECON*, 2014, pp. 5191–5195, doi: 10.1109/IECON.2014.7049290.

[13] J. Fernando and N. Kularatna, "Supercapacitor assisted surge absorber (SCASA) technique: Selection of supercapacitor and magnetic components," in *Proc. IEEE Energy Convers. Congr. Expo. (ECCE)*, 2014, pp. 1992–1996, doi: 10.1109/APEC42165.2021.9487254.

[14] S. U. Silva Thotabaddadurage, N. Kularatna, and D. A. Steyn-Ross, "Permeance based design and analysis of supercapacitor assisted surge absorber for magnetic component selection," *IEEE Trans. Ind. Electron.* **<AU: Please provide the year, volume number, issue number or a month and the page range. >**

[15] "UL 1449 third edition: SPD/TVSS Changes effective," Siemens Industry, Inc., White Paper, Sep. 29, 2009.

[16] S. U. Silva Thotabaddadurage, N. Kularatna, and D. A. Steyn-Ross, "Optimization of supercapacitor assisted surge absorber (SCASA) technique: A new approach to improve surge endurance using air-gapped ferrite cores," *Energies*, vol. 14, no. 14, p. 4337, Jul. 2021, doi: 10.3390/en14144337.

[17] S. T. Sadeeshvara Udayanga, N. Kularatna and D. A. Steyn-Ross, "Permeance based model for the coupled-inductor utilized in the supercapacitor assisted surge absorber (SCASA) and its experimental validation," in *Proc. 2nd IEEE Int. Conf. Ind. Electron. Sustain. Energy Syst. (IESES)*, Cagliari, Italy, 2020, pp. 267–272, doi: 10.1109/IESES45645.2020.9210663.

[18] S. T. Sadeeshvara Udayanga, S. Kokuhennadige, J. Fernando, N. Kularatna and D. A. SteynRoss, "Supercapacitor assisted surge absorber (SCASA) technique: Selection of magnetic components based on permeance," in *Proc. 36th IEEE Appl. Power Electron. Conf. Expo. (APEC)*, AZ, USA, 2021, pp. 2299–2304, doi: 10.1109/APEC42165.2021.9487254.

[19] S. T. Sadeeshvara Udayanga, N. Kularatna and D. A. Steyn-Ross, "Investigating the impact of ferrite magnetic cores on the performance of supercapacitor assisted surge absorber (SCASA) technique," in *Proc. 28th IEEE Int. Symp. Ind. Electron. (ISIE)*, Vancouver, BC, Canada, 2019, pp. 130–135, doi: 10.1109/ISIE.2019.8781402.

[20] S. U. Silva Thotabaddadurage, "Permeance based modelling, design and optimization of supercapacitor assisted surge absorber (SCASA)," Ph.D. thesis, The Univ. of Waikato, Hamilton, New Zealand, 2021.

PEM